Heliyon 10 (2024) e31843

Contents lists available at ScienceDirect

Heliyon

journal homepage: www.cell.com/heliyon

Research article

Multi-objective placement and sizing of energy hubs in energy networks considering generation and consumption uncertainties

Abdolhamid Rahideh, Mehrdad Mallaki *, Mojtaba Najafi, Abdolrasul Ghasemi

Electrical Engineering Department, Bushehr Branch, Islamic Azad University, Bushehr, Iran

ARTICLE INFO

Keywords:
Energy hub
Placement and sizing
Pareto optimization
Linear approximation model

ABSTRACT

This paper presents the placement and sizing of energy hubs (EHs) in electricity, gas, and heating networks. EH is a coordinator framework for various power sources, storage devices, and responsive loads. For simultaneous modeling of economic, operation, reliability, and flexibility indices, the proposed scheme is expressed as a three-objective optimization in the form of Pareto optimization based on the sum of weighted functions. The objective functions of this problem respectively minimize the planning cost of EHs (equal to the total cost of construction of hubs and their expected operating cost), the expected energy loss of the mentioned networks, and the expected energy not-supplied (EENS) of these networks in the case of an $N-1$ event. The problem is constrained by power flow equations and operation and reliability constraints of these network together with the EH planning and operation model, and flexibility constraints of the EHs. Then, to achieve unique optimal solution in the shortest possible time, a linear approximation model is extracted for the proposed scheme. Moreover, scenario-based stochastic programming (SBSP) is employed to model uncertainties of load, energy cost, renewable power, and accessibility of the mentioned network equipment. Finally, the obtained numerical results indicate the capability of the proposed scheme in enhancing the economic and flexibility situation of EHs and improving the reliability and operation status of energy networks along with achieving optimal planning and operation for EHs.

Nomenclature

A) *Variables*

$EENS$	Expected energy not-supplied (MWh)
E_E^{up}	Capacity of electrical energy storage (EES) expressed as the maximum storable energy (MWh)
E_T^{up}	Capacity of thermal energy storage (TES) expressed as the maximum storable energy (MWh)
EPC	Expected planning cost (sum of construction and operating cost) of EHs ($/year)
H_B^{up}	Capacity (maximum heat power) of the boiler in MW or per-unit (p.u.)
NEL	Expected energy losses of networks per year (p.u.)
P_R^{up}	Capacity (maximum active power) of renewable energy sources (RESs) in MW or p.u.
S_C^{up}	Capacity (maximum apparent power) of the combined heat and power (CHP) in MW or p.u.
G_C, H_C, P_C, Q_C	Gas, heat, active, and reactive power of the CHP (p.u.)
G_F, H_F, P_F, Q_F	Gas, heat, active, and reactive power flow through the distribution line (p.u.)
G_S, H_S, P_S, Q_S	Gas, heat, active, and reactive power flow through the distribution substation (p.u.)

(*continued on next page*)

* Corresponding author.
E-mail addresses: rahideh.hamid@yahoo.com (A. Rahideh), me.mallaki@iau.ac.ir (M. Mallaki).

https://doi.org/10.1016/j.heliyon.2024.e31843
Received 25 December 2023; Received in revised form 7 May 2024; Accepted 22 May 2024
Available online 23 May 2024

(*continued*)

G_E, H_E, P_E, Q_E	Gas, heat, active, and reactive power of the EH (p.u.)
G_{NS}, H_{NS}, P_{NS}	Gas, heat, and active demand not-supplied (p.u.)
G_B, H_B	Gas and heat power of the boiler (p.u.)
H_{CH}, H_{DIS}	Heat power of the TES during charge/discharge operating mode (p.u.)
H_{DR}, P_{DR}	Heat and active power of consumers collaborating in the demand response program (DRP) (p.u.)
P_{CH}, P_{DIS}	Active power of the EES during charge/discharge operating mode (p.u.)
P_R	Active power of the RES (p.u.)
T	Temperature (p.u.)
V, α	Voltage amplitude (p.u.) and voltage angle (rad)
χ	Pressure (p.u.)
ΔV	Voltage deviation (p.u)

B) *Constants*

B_F, G_F	Susceptance and conductance of electricity distribution line (p.u.)
CF	Coincidence factor
Du	Number of outage days
A_E, A_H, A_G	Incidence matrices of EHs-electrical buses, EHs-heat nodes, and EHs-gas nodes
B_E, B_H, B_G	Incidence matrices of electricity buses-lines, heat nodes-pipelines, and gas nodes-pipelines
$E_E^{\max}$, $E_T^{\max}$	Maximum energy storage in the EES and TES (MWh or p.u.)
G_L, H_L, P_L, H_L	Gas, heat, active and reactive demand (p.u.)
G_F^{up}, G_S^{up}	Maximum gas power flow on the gas distribution station and pipeline (p.u.)
$H_B^{\max}$	Maximum heat power of the boiler (p.u.)
H_F^{up}, H_S^{up}	Maximum heat power flow on the heat distribution station and pipeline (p.u.)
C_B, C_C, C_E, C_T, C_R	Cost of the boiler, combined heat and energy (CHP), EES, TES, and RES per year ($/year)
$P_R^{\max}$	Maximum active power of the RES (p.u.)
$S_C^{\max}$	Maximum apparent power of the CHP (p.u.)
S_F^{up}, S_S^{up}	Maximum apparent power flow through the electricity distribution line and substation (p.u.)
T^{lo}, T^{up}	Minimum and maximum temperature (p.u.)
V^{lo}, V^{up}	Minimum and maximum voltage amplitude (p.u.)
ς_F, ξ_F	Heat and gas constants of the distribution pipeline
ϖ	Ratio between maximum heat power and maximum active power of the CHP
η_{CH}, η_{DIS}	Charge/discharge efficiency of the storage
η_B	Efficiency of the boiler
η_T, η_L, η_H	Efficiency of the turbine, losses, and heat of the CHP
γ_E, γ_H, γ_G	Energy price in electricity, heat, and gas energy networks ($/MWh)
ρ	Probability of occurrence of a scenario
χ^{lo}, χ^{up}	Minimum and maximum pressure (p.u.)
τ_{CH}, τ_{DIS}	Charge/discharge time of the storage system
ψ	Participation rate of consumers in the DRP
υ, ν	Ratio between minimum and maximum energy of the storage, and the ratio between the initial energy and maximum energy of the storage
ΔF	Flexibility tolerance (p.u.)
$\Delta\varphi$	Angle deviation (rad)

C) *Indices*

e, g, t	Electrical bus, gas node, heat node
m	A member of the Pareto front
n_m	Number of members in the Pareto front
i	EH
t	Operation hour
w	A scenario obtained from the scenario-reduction method
s	Line segment in the piecewise linearization technique
k	Sides of a regular polygon
l	Electrical bus, or gas node, or heat node

1. Introduction

1.1. Motivation

Currently, thanks to advances in environment-friendly power generation and storage technology, these technologies are widely used more than ever. Renewable energy sources (RES), like wind turbines (WTs) and photovoltaic systems (PVs), cause very negligible environmental impact. In addition, as such resources impose low operating costs they can be located in demand side and present green energy besides enhancing the operation status of the whole system [1]. Speaking of clean energy resources, distribution generation (DG) units, e.g. microturbine, fuel cell, and combined heat and energy (CHP) plants, have found their developed application within

power systems because of low pollution they produce. Operation, reliability, resilience, and flexibility indicators of the network can be enhanced via employing RESs on the demand side by controlling the output generation power [2,3]. Another solution proposed for enhancing these indicators is the adoption of energy storage systems (ESSs) and demand response programs (DRPs), which help smooth the power curve of the system [1]. Thus, it would be very suitable if an operator could integrate and coordinate system elements so that various indicators of the system are improved together with supplying green energy across the grid. To this end, some studies suggest the use of virtual power plant (VPP), microgrids (MGs), and energy hubs (EHs) [4]. The collaborated adoption of RESs and ESSs would enhance the flexibility. However, the single use of RESs may deteriorate flexibility situation [5]. Yet, one should note that in the case of employing EHs, electricity, gas, and heat energy can be managed at the same time, thus increasing the efficiency [6]. Consequently, an acceptable integration and arrangement of such equipment need to be advised. Regarding that the system designer and operator cannot exploit an arbitrary number of power sources, ESS devices, and responsive loads, the optimal placement and sizing of these equipment would assist achieving the favorable system status in terms of technical and economic indicators. To reach this aim, we can again employ EHs consisting of power sources, ESS, and responsive loads, which help improve different indicators of the system.

1.2. Literature review

There is a huge research behind placement and sizing of power sources and energy storage. The following reviews some of the background study. Ref. [7] develops a method for optimal siting of DGs (including WTs and PVs) together with capacitor banks using technical and economic indicators. To take the innate randomness of WTs and PVs into account, the study adopts a Monte Carlo method and diagonal bank Copula model, integrates them and uses the extracted data of wind, irradiance, and demand. The authors also employ genetic algorithm to solve the formulated optimization problem. Optimal siting and sizing of WTs in both deterministic and probabilistic cases has also been analyzed hoping to reduce power loss, flatten the voltage profile, and enhance system stability [8]. To this end, the β-chaotic sequence spotted hyena optimizer was used. In other study, distributed battery ESSs are robustly scheduled so that flexibility is enhanced. In this work, the difference between costs (caused by battery scheduling, degradation, and operation) and revenues (obtained from selling battery power) are minimized by using a deterministic model of the problem. Robust optimization is incorporated to model uncertainty quantities (such as predicted active/reactive demand, energy price, charge/discharge price, and RESs power). A novel resiliency framework for distribution system is adopted in Ref. [9] to enhance resiliency in the event of unwanted natural events like earthquake and flood. The model finds the minimum cost of planning and operation, as well as the minimum values of load shedding and repair and maintenance cost caused by the events. The problem is constrained by planning model, linearized operation equations, and rearrangement formulae of the system. Optimal placement, selection, and operation of battery-type ESS and renewable DGs has been addressed in Ref. [10], where the problem is expressed as a mixed-integer nonlinear programming (MINLP) model that is solved using a planning-operation decomposition method. The suggested approach includes two subproblems, one for planning and the other for operation purposes. The former is associated with the placement and selection of the ESSs and DGs, while the latter attempts to reach the optimal operation scheduling of the batteries.

One approach to providing financial benefit and supply higher energy is the utilization of EHs for power sources, ESS, and responsive loads and their simultaneous and collaborative management. This helps to successfully plan and operate these devices in the form of EHs so that different indicators of the system are enhanced at the same time without any compromise [11]. There is a substantial amount of research concerning the operation of EHs. Ref. [12] proposes a strategy for EHs aiming to find the optimal operation of MGs and minimize the operating cost while taking the environmental challenges into account. The adopted EH in this study uses a combined cooling, heating, power (CCHP) system consisting of WTs and PVs. The energy storage resources of the EH include an ice storage conditioner (ISC) system and an ESS. Coordinated energy management of EHs located at different networks is introduced in Ref. [13] using the cooperation of EHs in day-ahead energy market. The objective function of the management problem maximizes EHs' profit constrained by linear networks and EHs limitations. The proposed model considers uncertainty parameters as well. The problem is mathematically expressed in the form of a scenario-based stochastic model. Monte Carlo Simulation (MCS) is used

Table 1
Taxonomy of recent works in the area.

Ref.	Model of placement and sizing of EH	Indices				Planning-operation model of EH
		Economic	Operation	Reliability	Flexibility	
[7]	No	Yes	Yes	No	No	No
[8]	No	Yes	Yes	Yes	No	No
[9]	No	Yes	Yes	No	No	No
[10]	No	Yes	Yes	No	No	No
[11]	No	Yes	Yes	No	No	No
[12]	No	No	Yes	No	No	No
[13]	No	Yes	Yes	No	No	No
[14]	No	Yes	Yes	No	No	No
[15]	No	No	Yes	No	No	No
[16]	No	Yes	Yes	No	No	No
[17]	No	Yes	Yes	No	No	No
Proposed method	**Yes**	**Yes**	**Yes**	**Yes**	**Yes**	**Yes**

to generate scenarios and the fast backward/forward scenario reduction method is adopted to limit the number of scenarios. Ref. [14] proposes a stochastic structure for optimal operation of EHs consisting of energy converters and ESSs. The structure significantly impacts the bidding strategy of smart devices. Random scenarios are also generated to model the uncertainties associated with energy price, wind speed, and irradiance. A robust model based on information-gap decision theory (IGDT) is used in Ref. [15] to manage multicarrier energy system. The first step is to state a deterministic model of the problem, in which the total cost of EHs is minimized. Problem constraints include power flow equations and limitations of indicators related to electricity, gas, and heating networks, and some other parameters. The IGDT-based robust optimization solves the problem by dealing with the uncertainties. Energy management of EHs connected to electricity, gas, and heating network is stated in Ref. [16], where the role of an EH is to coordinate DGs and ESSs. Uncertainties are modeled by using an adaptive robust optimization method. A list of some studies related to placement and sizing of EHs is reported in Table 1.

1.3. Research gaps

According to the background review and Table 1, one can pinpoint the following research gaps to fill in the realm of operation and planning of power sources, ESSs, and responsive loads using grid-connected structure of EHs.

- Most of the works focus on allocation and/or sizing of power sources, ESSs, and responsive loads. Some deal with simultaneous planning modeling of the equipment also these elements are placed at different buses of the network. Nonetheless, when the equipment is incorporated in the form of EHs, VPPs, or other combined models, more advantages are achieved compared to that of their separate management [11]. This has been validated in Ref. [13] as well. Unfortunately, the allocation and finding the proper size of these elements in the form of EH need more attention and deeper research should be done.
- It is noteworthy that the number of EHs is generally low in energy networks. Therefore, in order to achieve the desired economic and technical status in these networks, it is necessary to obtain the results of optimal planning for EHs along with achieving their optimal operation status. Note, however, that most research has focused on the operation model of EHs in energy networks, and less on the combined model of operation and planning of grid-connected EHs.
- In most studies, economic and operational indices in EH optimization problems in energy networks have been considered. However, in an energy network, there are various economic and technical indices such as operation, reliability, flexibility, and other factors, where improving the status of one index does not ensure improving the status of other indices. For example, to minimize the cost of purchasing energy of energy networks, EHs need to inject high power into the network. Nonetheless, in these conditions, energy losses, which is an operation index, may not be minimized and show a high value. Therefore, it is expected that to address this issue, simultaneous modeling of several indices is applied to the problem.

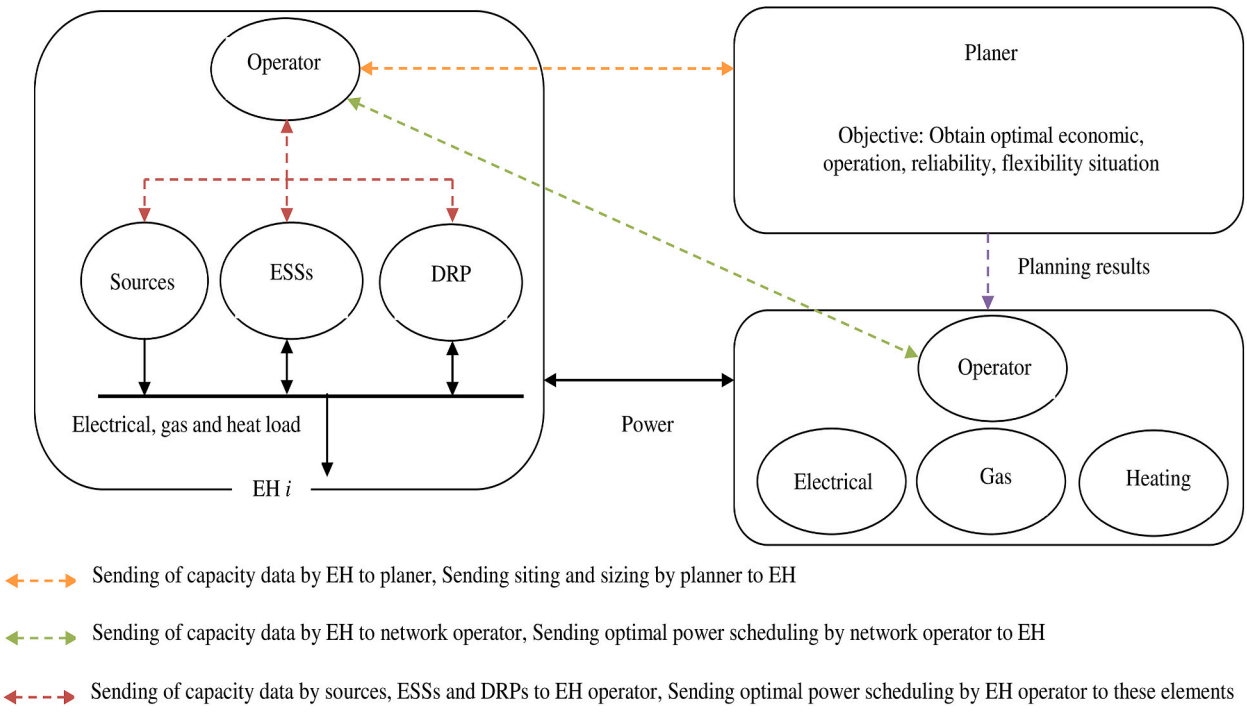

Fig. 1. Planning-operation framework of grid-connected EHs in energy networks.

1.4. Contributions

To address the research gaps mentioned in the previous section, this paper as Fig. 1 finds the location and capacity of power sources and ESSs in EHs framework, which provides load responsiveness in electricity, gas, and heating networks. To structure the proposed design, three-objective optimization is used aiming to minimize the planning cost (capital and operating cost) of EHs, expected energy loss of networks, and EENS in the case of an $N-1$ event. The problem is constrained by optimal power flow equations, reliability index, and operation and planning models of power sources and ESSs. An integrated single-objective model is obtained by using the Pareto optimization and sum of weighted functions. The problem is stated as MINLP. To reduce the computational time and burden, the problem is solved using a linear approximation model and unique optimal solution is obtained. The design is subject to uncertainties associated with load, energy price, renewable power, and accessibility of system elements. The present paper adopts stochastic optimization based on Combination of Mont Carlo simulation (MCS) and Kantorovich method (KM) to find the optimal solution. Innovations of the paper include the following items.

- Finding the location and size of power sources and ESSs in an EHs framework that consists of responsive loads of electricity, gas, and heating networks;
- Modeling the operation and planning of EHs at the same time so that the optimal location, capacity, and operation status of EHs are found; and
- Modeling economic, operation, reliability and flexibility indicators of the mentioned networks as a multi-objective optimization problem.

1.5. Paper organization

Different sections of the paper are organized as follows. Multi-objective model of EHs planning is described in Section 2. Section 3 provides a single-objective model based on Pareto optimization and uncertainty parameters are modeled. Results are given in Section 4 in detail and Section 5 concludes the paper.

2. Multi-objective planning of grid-connected EHs

2.1. Non-linear model

Finding the optimal location of size of power sources and ESSs as grid-connected EHs considering DRP is directly related to economic and technical indicators of electricity, gas, and heating networks. An optimization problem with three different objective functions is structured in the proposed design to minimize the planning cost of EHs, network energy loss, and EENS of these networks. Constraints of the problem include optimal power flow equations, reliability index, planning and operation models of EHs, and flexibility status of EHs. The suggested design is thoroughly described as follows.

A) *Objective functions*: Economic, operation, reliability, and flexibility indicators of EHs and energy networks are modeled through an optimization problem with three objectives. Equation (1) describes the objectives, in which the planning cost of power sources and ESSs; total capital cost of CHPs, boilers, RESs, electrical energy storages (EESs), and thermal energy storages (TESs) per year; and predicted operating cost of EHs are minimized. The operating cost includes the cost of purchasing energy by EHs from electricity, gas, and heating networks [13]. Negative power of EH means that the EH supplies power to the upstream grid and gains revenue. The predicted energy loss of electricity, gas, and heating networks is calculated and minimized in Eq. (2) [13]. The main goal of seeking optimized site and size of EHs is to improve operation indices. To this end, the best place for EHs is demand sides. Thereby, during a fault that an $N-1$ event may happen, the rate of outage will reduce thanks to EHs. Equation (3) expresses the formulation to minimize the EENS value of electricity, gas, and heating networks in the case of an $N-1$ event [2–17]. If this value is small, the outage rate is small. As this is an indicator of reliability, EENS is set as a reliability index [2].

$$\min \quad EPC = \sum_{i} \left(C_{C\,i} S_{C\,i}^{up} + C_{B\,i} H_{B\,i}^{up} + C_{R\,i} P_{R\,i}^{up} + C_{E\,i} E_{E\,i}^{up} + C_{T\,i} E_{T\,i}^{up} \right) + 365 \times CF \times \sum_{i,t,w} \rho_w \left(\gamma_{E\,t,w} P_{E\,i,t,w} + \gamma_{H\,t,w} H_{E\,i,t,w} + \gamma_{G\,t,w} G_{E\,i,t,w} \right) \tag{1}$$

$$\min \quad \mathrm{NEL} = 365 \times \mathrm{CF} \times \begin{pmatrix} \sum_{e,t,w} \rho_w \left(P_{S\,e,t,w} - P_{L\,e,t,w} + \sum_{i} A_{E\,e,i} P_{E\,i,t,w} \right) + \\ \sum_{h,t,w} \rho_w \left(H_{S\,h,t,w} - H_{L\,h,t,w} + \sum_{i} A_{H\,h,i} H_{E\,i,t,w} \right) + \\ \sum_{g,t,w} \rho_w \left(G_{S\,g,t,w} - G_{L\,g,t,w} + \sum_{i} A_{G\,g,i} G_{E\,i,t,w} \right) \end{pmatrix} \tag{2}$$

$$\min \quad EENS = du \times CF \times \left(\sum_{w} \rho_w \left(\sum_{e,t} P_{NS\,e,t,w} + \sum_{h,t} H_{NS\,h,t,w} + \sum_{g,t} G_{NS\,g,t,w} \right) \right) \tag{3}$$

B) *Constraints of energy networks*: Power flow constraints of electricity, gas, and heating networks, (4)–(11) [13,15,16], operating limits of the mentioned networks, (12)–(20) [6,13], and reliability boundaries of these networks, (21)–(23) are given in this part [2]. Equations (4)–(7) describe the active-reactive power balance at electrical network buses, heating power balance at heating network nodes, and gas power balance at gas network nodes. Active and reactive power flow on electricity distribution lines together with heating and gas power flows on distribution pipes are given in (8)-(11). These equations show the nonlinear and real model of power flow in these networks. Furthermore, operating constraints of electricity, gas, and heating networks in this problem are related to allowable ranges of electrical bus voltage (12), heating node temperature (13), gas node pressure (14), and capacity of electrical, gas and heating distribution lines and substation (15)–(20). The constraints related to the maximum apparent power flow through distribution lines and substations are represented in (15)-(16). Constraints related to the maximum heating (gas) power flowing through the heating (gas) pipelines and station are shown in (17)-(18)/(19)–(20). Equations (4)–(20) assume that energy networks are connected to their corresponding upstream network via a distribution substation located at the slack bus. This means that, the distribution substation is accessible only at the slack bus (node); hence, variables P_S, Q_S, H_S, and G_S have values for this bus and are zero for other buses (nodes). Parameter u denotes the availability of energy networks equipment including lines, pipelines, and distribution stations during an $N-1$ event. This parameter is either 0 or 1. It is 0 if the equipment is not in the network; otherwise, it is 1. Constraints associated with active, heating, and gas load are represented in Eqs. (21)–(23). According to subsection 2.1.A, EENS is a reliability index, as provided in (3), which is proportional to the load not-supplied (LNS). As a result, Eqs. (21)–(23) will represent reliability constraints.

$$P_{NS\ e,t,w} + P_{S\ e,t,w} + \sum_i A_{E\ e,i} P_{E\ i,t,w} - \sum_l B_{E\ e,l} P_{F\ e,l,t,w} = P_{L\ e,t,w} \quad \forall e,t,w \tag{4}$$

$$\mathrm{Q_{NS\ e,t,w}} + \mathrm{Q_{S\ e,t,w}} + \sum_{\mathrm{i}} \mathrm{A_{E\ e,i}} \mathrm{Q_{E\ i,t,w}} - \sum_{\mathrm{l}} \mathrm{B_{E\ e,l}} \mathrm{Q_{F\ e,l,t,w}} = \mathrm{Q_{L\ e,t,w}} \quad \forall \mathrm{e,t,w} \tag{5}$$

$$H_{NS\ h,t,w} + H_{S\ h,t,w} + \sum_i A_{H\ h,i} H_{E\ i,t,w} - \sum_l B_{H\ h,l} H_{F\ h,l,t,w} = H_{L\ h,t,w} \quad \forall h,t,w \tag{6}$$

$$G_{NS\ g,t,w} + G_{S\ g,t,w} + \sum_i A_{G\ g,i} G_{E\ i,t,w} - \sum_l B_{G\ g,l} G_{F\ g,l,t,w} = G_{L\ g,t,w} \quad \forall g,t,w \tag{7}$$

$$P_{F\ e,l,t,w} = \left(G_{F\ \ e,l} \left(V_{e,t,w}\right)^2 - V_{e,t,w} V_{l,t,w} \left\{ \begin{matrix} G_{F\ \ e,l} \cos\left(\alpha_{e,t,w} - \alpha_{l,t,w}\right) + \\ B_{F\ \ e,l} \sin\left(\alpha_{e,t,w} - \alpha_{l,t,w}\right) \end{matrix} \right\} \right) u_{eF\ e,l,w} \quad \forall e,l,t,w \tag{8}$$

$$Q_{F\ e,l,t,w} = \left(- B_{F\ \ e,l} \left(V_{e,t,w}\right)^2 + V_{e,t,w} V_{l,t,w} \left\{ \begin{matrix} B_{F\ \ e,l} \cos\left(\alpha_{e,t,w} - \alpha_{l,t,w}\right) - \\ G_{F\ \ e,l} \sin\left(\alpha_{e,t,w} - \alpha_{l,t,w}\right) \end{matrix} \right\} \right) u_{eF\ e,l,w} \quad \forall e,l,t,w \tag{9}$$

$$\mathrm{H_{F\ h,l,t,w}} = \varsigma_{\mathrm{F\ h,l}} \left(\mathrm{T_{h,t,w}} - \mathrm{T_{l,t,w}}\right) \mathrm{u_{hF\ h,l,w}} \quad \forall \mathrm{h,l,t,w} \tag{10}$$

$$G_{F\ g,l,t,w} = u_{gF\ g,l,w} \xi_{F\ g,l} sign\left(\chi_{g,t,w}, \chi_{l,t,w}\right) \sqrt{sign\left(\chi_{g,t,w}, \chi_{l,t,w}\right) \left(\left(\chi_{g,t,w}\right)^2 - \left(\chi_{l,t,w}\right)^2 \right)} \quad \forall g,l,t,w \tag{11}$$

$$V_e^{lo} \le V_{e,t,w} \le V_e^{up} \quad \forall e,t,w \tag{12}$$

$$\mathrm{T_h^{lo}} \le \mathrm{T_{h,t,w}} \le \mathrm{T_h^{up}} \quad \forall \mathrm{h,t,w} \tag{13}$$

$$\chi_g^{lo} \le \chi_{g,t,w} \le \chi_g^{up} \quad \forall g,t,w \tag{14}$$

$$\sqrt{\left(P_{F\ e,l,t,w}\right)^2 + \left(Q_{F\ e,l,t,w}\right)^2} \le S_{F\ e,l}^{up} \quad \forall e,l,t,w \tag{15}$$

$$\sqrt{\left(P_{S\ e,t,w}\right)^2 + \left(Q_{S\ e,t,w}\right)^2} \le u_{eS\ e,w} S_{S\ e}^{up} \quad \forall e = \text{Slack bus},t,w \tag{16}$$

$$-H_{F\ h,l}^{up} \le H_{F\ h,l,t,w} \le H_{F\ h,l}^{up} \quad \forall h,l,t,w \tag{17}$$

$$-u_{hS\ h,w} H_{S\ h}^{up} \le H_{S\ h,t,w} \le u_{hS\ h,w} H_{S\ h}^{up} \quad \forall h = \text{Slack node},t,w \tag{18}$$

$$-G_{F\ g,l}^{up} \le G_{F\ g,l,t,w} \le G_{F\ g,l}^{up} \quad \forall g,l,t,w \tag{19}$$

$$-u_{gS\ g,w} G_{S\ g}^{up} \le G_{S\ g,t,w} \le u_{gS\ g,w} G_{S\ g}^{up} \quad \forall g = \text{Slack node},t,w \tag{20}$$

$$0 \le P_{NS\ e,t,w} \le P_{L\ e,t,w} \quad \forall e,t,w \tag{21}$$

$$0 \le H_{NS\ h,t,w} \le H_{L\ h,t,w} \quad \forall h,t,w \tag{22}$$

$$0 \le G_{NS\ g,t,w} \le G_{L\ g,t,w} \quad \forall g,t,w \tag{23}$$

C) *Operation and planning model of EHs*: Constraints (24)–(47) show the planning and operation status of power sources and ESSs in EHs that include DRPs. The end-users are assumed to participate in DRPs at parts of the network that an EH is present. In this part, constraints (24)–(27) describe the active, reactive, heating, and gas power balance equations of the EH, in which, CHP, RES, DRP, and EES (including stationary storages such as batteries) can help the electricity sector to manage active power of the EH. CHP is the only option to control reactive power of the EH. RESs and EESs, based on the IEEE 1547 standard, are active only at the electrical energy (active power) management sector [18]. CHP, boiler, TES, and DRP assist to control heating power of EHs. As per (27), EH is assumed to use merely the gas network to extract electrical and heating energy of the boiler and CHP. The rest of constraints related to other equipment are provided in (28)-(47). Equations (28)–(32) describe the planning and operating model of the CHP [19], in which heating power production by CHP and its gas consumption are given in (28)-(29), both of which are a factor of CHP active power. Constraints (30)–(31) present the output capacity limit of CHP, which show the maximum apparent power and maximum controllable heating power of the CHP, respectively. The planning model of CHP is given by (32), where if the size variable of CHP, i.e. S_C^{up}, is nonzero (zero), the construction of CHP in the EH is (not) essential from economic and technical aspects. Operating constraints of the boiler are modeled in (33)-(35) [13] that describe boiler gas power, its output capacity range, and its size limit in the EH. If $H_B^{up} \neq 0$ ($H_B^{up} = 0$), embedding a boiler in the EH is (not) mandatory. Operating and planning models of RESs are given in (36)-(37). According to (36), active power output of RESs is equal to its output power (φ_R is between 0 and 1) multiplied by RESs size [1]. Equation (37) gives the size limit of RESs. In these constraints, if $P_R^{up} \neq 0$ ($P_R^{up} = 0$), the construction of RESs in the EH is (not) beneficial from economic and technical points of view.

Constraints (38)–(41) address the planning and operating model of EESs [20]. Limitation of charge rate, discharge rate, and energy storage in ESSs are shown by (38)-(40). Equation (41) gives the size limit of the EESs, which represents the maximum energy that can be stored in EESs. A similar model, (38)–(41), is constructed for TESs in constraints (42)–(45), except that heating power variables of TESs substitute active power variables. In (38)-(45), if E^{up} is not zero, the placement of storages in the EH can be justified from economic and technical viewpoints. A model of DRP is given in constraints (46)–(47) for electrical and heating energy consumers [1, 21]. This model is based on an incentive model, in which end-users can decrease or increase the consumption rate using the price signal. To provide more details, during high energy prices (corresponding to peak load), end-users consume low energy, while during low energy prices (off-peak load), they consume higher. Nonetheless, customers tend to meet the demand during the operating horizon of the EH. As a result, this model gives a shift in energy consumption from peak to off-peak hours. This lowers the operating cost of EHs (1). Constraint (46) shows power changes applied by consumers in the DRP. Moreover, constraint (47) guarantees that decrease in energy consumption during peak hours is met by the EH during off-peak hours [21].

Finally, the flexibility models of EHs in the electrical and thermal sections are expressed in (48) and (49), respectively. Note that the presence of RESs makes the DA and RT operation results to be different [4]. This is due to the uncertainty in their active power generation. This results in reduced EH flexibility in the electrical sector [4]. To compensate for that, flexibility sources such as storage and DRP should reduce the fluctuations of EH active power in RT operation compared to DA operation [5]. To derive this, one can mathematically minimize the deviation of the active power of EH in a scenario w with respect to the scenario corresponding to the deterministic model (here the first scenario is assumed) [22]. This is the case in (48), so in this equation, if the flexibility tolerance (ΔF) goes to zero, the EH flexibility will go to 100 % improvement. In addition, the thermal power of CHP is not independent of its active power. Therefore, it is possible that the results of RT and DA operation of EH in the thermal sector are not the same [19]. Thus, DRP, TES, and boiler will be responsible for improving flexibility in this sector, so a model similar to that of the electrical section is considered in (49) for the EH thermal sector.

$$P_{E\ i,t,w} = P_{C\ i,t,w} + P_{R\ i,t,w} + P_{DR\ i,t,w} + \left(P_{DIS\ i,t,w} - P_{CH\ i,t,w}\right) - P_{L\ i,t,w} \quad \forall i,t,w \tag{24}$$

$$Q_{E\ i,t,w} = Q_{C\ i,t,w} - Q_{L\ i,t,w} \quad \forall i,t,w \tag{25}$$

$$H_{E\ i,t,w} = H_{C\ i,t,w} + H_{B\ i,t,w} + H_{DR\ i,t,w} + \left(H_{DIS\ i,t,w} - H_{CH\ i,t,w}\right) - H_{L\ i,t,w} \quad \forall i,t,w \tag{26}$$

$$G_{E\ i,t,w} = -G_{C\ i,t,w} - G_{B\ i,t,w} - G_{L\ i,t,w} \quad \forall i,t,w \tag{27}$$

$$H_{C\ i,t,w} = P_{C\ i,t,w} \frac{(1-\eta_T-\eta_L)\eta_H}{\eta_T} \quad \forall i,t,w \tag{28}$$

$$G_{C\ i,t,w} = P_{C\ i,t,w} \frac{1}{\eta_T} \quad \forall i,t,w \tag{29}$$

$$\sqrt{\left(P_{C\,i,t,w}\right)^2+\left(Q_{C\,i,t,w}\right)^2}\le S_{C\,i}^{up}\quad \forall i,t,w \tag{30}$$

$$-\varpi_i S_{C\,i}^{up}\le H_{C\,i,t,w}\le \varpi_i S_{C\,i}^{up}\quad \forall i,t,w \tag{31}$$

$$0\le S_{C\,i}^{up}\le S_{C\,i}^{max}\quad \forall i \tag{32}$$

$$G_{B\,i,t,w}=H_{B\,i,t,w}\frac{1}{\eta_B}\quad \forall i,t,w \tag{33}$$

$$-H_{B\,i}^{up}\le H_{B\,i,t,w}\le H_{B\,i}^{up}\quad \forall i,t,w \tag{34}$$

$$0\le H_{B\,i}^{up}\le H_{B\,i}^{max}\quad \forall i \tag{35}$$

$$P_{R\,i,t,w}=\varphi_{R\,i,t,w}P_{R\,i}^{up}\quad \forall i,t,w \tag{36}$$

$$0\le P_{R\,i}^{up}\le P_{R\,i}^{max}\quad \forall i \tag{37}$$

$$0\le P_{CH\,i,t,w}\le \frac{E_{E\,i}^{up}}{\tau_{CH\,i}}\quad \forall i,t,w \tag{38}$$

$$0\le P_{DIS\,i,t,w}\le \frac{E_{E\,i}^{up}}{\tau_{DIS\,i}}\quad \forall i,t,w \tag{39}$$

$$\upsilon_i E_{E\,i}^{up}\le v_i E_{E\,i}^{up}+\sum_{o=1}^{t}\left(\eta_{CH\,i}P_{CH\,i,o,w}-\frac{1}{\eta_{DIS\,i}}P_{DIS\,i,o,w}\right)\le E_{E\,i}^{up}\quad \forall i,t,w \tag{40}$$

$$0\le E_{E\,i}^{up}\le E_{E\,i}^{max}\quad \forall i \tag{41}$$

$$0\le H_{CH\,i,t,w}\le \frac{E_{T\,i}^{up}}{\tau_{CH\,i}}\quad \forall i,t,w \tag{42}$$

$$0\le H_{DIS\,i,t,w}\le \frac{E_{T\,i}^{up}}{\tau_{DIS\,i}}\quad \forall i,t,w \tag{43}$$

$$\upsilon_i E_{T\,i}^{up}\le v_i E_{T\,i}^{up}+\sum_{o=1}^{t}\left(\eta_{CH\,i}H_{CH\,i,o,w}-\frac{1}{\eta_{DIS\,i}}H_{DIS\,i,o,w}\right)\le E_{T\,i}^{up}\quad \forall i,t,w \tag{44}$$

$$0\le E_{T\,i}^{up}\le E_{T\,i}^{max}\quad \forall i \tag{45}$$

$$-\psi_i P_{L\,i,t,w}\left(\text{or } H_{L\,i,t,w}\right)\le P_{DR\,i,t,w}\left(\text{or } H_{DR\,i,t,w}\right)\le \psi_i P_{L\,i,t,w}\left(\text{or } H_{L\,i,t,w}\right)\quad \forall i,t,w \tag{46}$$

$$\sum_t P_{DR\,i,t,w}\left(\text{or } H_{DR\,i,t,w}\right)=0\quad \forall i,w \tag{47}$$

$$-\Delta F\le P_{E\,i,t,w}-P_{E\,i,t,w=1}\le \Delta F\quad \forall i,t,w \tag{48}$$

$$-\Delta F\le H_{E\,i,t,w}-H_{E\,i,t,w=1}\le \Delta F\quad \forall i,t,w \tag{49}$$

2.2. Linear approximation formulation

The problem (1)-(49) has a MINLP model. Its solvers provide different solutions, so the optimal solution obtained has a low reliability [16]. Also, a high computational time is required to solve it, where the optimal solution in cases with high data volume studies may not be obtained [16]. To address this issue, a linear approximation model is obtained for the proposed scheme. Its solvers are able to extract a unique optimal solution at low computational time. To linearize the proposed scheme, note that the voltage deviation at both ends of an electrical distribution line is generally less than 6° [9,20]. Hence, the expressions $\cos\left(\alpha_{e,t,w}-\alpha_{l,t,w}\right)$ and $\sin\left(\alpha_{e,t,w}-\alpha_{l,t,w}\right)$ are approximated to 1 and $\left(\alpha_{e,t,w}-\alpha_{l,t,w}\right)$, respectively. Also, the voltage amplitude should be maintained between 0.9 and 1.1 p.u., so it is close to 1 p.u [13]. Therefore, V can be expressed as $1+\Delta V$, where ΔV represents the voltage deviation and its value is much less than 1 p.u. Then, ignoring the small values of ΔV^2, $\Delta V_{en}\Delta V_k$, and $\Delta V\times(\alpha_e - \alpha_l)$, constraints (8) and (9) can be expressed in the form of (50) and (51), respectively, which have a linear format:

$$P_{F\ e,l,t,w} = \left(G_{F\ \ e,l}\left(\Delta V_{e,t,w} - \Delta V_{l,t,w}\right) - B_{F\ \ e,l}\left(\alpha_{e,t,w} - \alpha_{l,t,w}\right)\right)u_{eF\ e,l,w} \quad \forall e,l,t,w \tag{50}$$

$$P_{F\ e,l,t,w} = \left(-B_{F\ \ e,l}\left(\Delta V_{e,t,w} - \Delta V_{l,t,w}\right) - G_{F\ \ e,l}\left(\alpha_{e,t,w} - \alpha_{l,t,w}\right)\right)u_{eF\ e,l,w} \quad \forall e,l,t,w \tag{51}$$

In the above formulation, the voltage deviation variable replaced the voltage amplitude, so constraint (12) is updated as follows:

$$V_e^{lo} - 1 \le \Delta V_{e,t,w} \le V_e^{up} - 1 \quad \forall e,t,w \tag{52}$$

To line constraint (11), the expression $\sqrt{sign\left(\chi_{g,t,w},\chi_{l,t,w}\right)\left(\left(\chi_{g,t,w}\right)^2 - \left(\chi_{l,t,w}\right)^2\right)}$ is first considered with an auxiliary variable $\beta_{g,l,t,w}$. In these conditions, we have $\beta_{g,l,t,w} = sign\left(\chi_{g,t,w},\chi_{l,t,w}\right)\left(\left(\chi_{g,t,w}\right)^2 - \left(\chi_{l,t,w}\right)^2\right)$. This relationship can be transformed into a linear relationship using the conventional piecewise linearization technique [13]. In this method, the variables β and χ can be expressed as $\beta = \sum_s \Delta\beta_s$ and $\chi = \chi^{lo} + \sum_s \Delta\chi_s$, respectively, where $\Delta\beta$ and $\Delta\chi$ are known as the deviations of the variables β and χ, and s is the index of each linear segment. In this case, the expressions β^2 and χ^2 can be written as $\beta = \sum_s ls_s^{\beta}\Delta\beta_s$ and $\chi = \left(\chi^{lo}\right)^2 + \sum_s ls_s^{\chi}\Delta\chi_s$, respectively, where ls^{β} and ls^{χ} represent the slope of the linear piecewise in the linearization of β^2 and χ^2, respectively [13]. Therefore, in these conditions, the linearized relations equivalent to constraint (11) can be written as follows:

$$G_{F\ g,l,t,w} = u_{gF\ g,l,w}\xi_{F\ g,l}\beta_{g,l,t,w} \quad \forall g,l,t,w \tag{53}$$

$$\Delta\beta_{g,l,t,w,s} = \mathrm{sign}\left(\chi_{g,t,w},\chi_{l,t,w}\right)\frac{ls_s^{\chi}}{ls_s^{\beta}}\left(\Delta\chi_{g,t,w,s} - \Delta\chi_{l,t,w,s}\right) \quad \forall g,t,w,s \tag{54}$$

$$\beta_{g,l,t,w} = \sum_s \Delta\beta_{g,l,t,w,s} \quad \forall g,t,w,s \tag{55}$$

$$\chi_{g,t,w} = \chi_g^{lo} + \sum_s \Delta\chi_{g,t,w,s} \quad \forall g,t,w \tag{56}$$

In (53), the G_F function is expressed in terms of β, then the linearized model of the expression $\beta_{g,l,t,w} = sign\left(\chi_{g,t,w},\chi_{l,t,w}\right)\left(\left(\chi_{g,t,w}\right)^2 - \left(\chi_{l,t,w}\right)^2\right)$ appears in constraint (54). In the following, the linear model of variables β and χ are presented in constraints (55) and (56), respectively.

The nonlinear constraints (15)–(16) and (30) are in the form of a circular plane with radius S with the center point of origin in the PQ coordinates. To express a linear relation for it, this plane can be approximated to a regular polygon plane [6,20]. On this plane, the sides have a linear formulation as $P \times \cos(k \times \Delta\varphi) + Q \times \sin(k \times \Delta\varphi) = S$, with k denoting a side and $\Delta\varphi$ denoting the angle deviation. The angle deviation is also $360/n_S$, where n_S represents the total number of sides. Next, the plane resulting from each side is given as $P \times \cos(k \times \Delta\varphi) + Q \times \sin(k \times \Delta\varphi) \le S$, which expresses a regular polygon plane for all sides [20]. Therefore, the linear constraints of constraints (15)–(16) and (30) are written as follows:

$$P_{F\ e,l,t,w}\cos(k \times \Delta\varphi) + Q_{F\ e,l,t,w}\sin(k \times \Delta\varphi) \le S_{F\ e,l}^{up} \quad \forall e,l,t,w,k \tag{57}$$

$$P_{S\ e,t,w}\cos(k \times \Delta\varphi) + Q_{S\ e,t,w}\sin(k \times \Delta\varphi) \le u_{eS\ e,w}S_{S\ e}^{up} \quad \forall e = \text{Slack bus},t,w,k \tag{58}$$

$$P_{C\ i,t,w}\cos(k \times \Delta\varphi) + Q_{C\ i,t,w}\sin(k \times \Delta\varphi) \le S_{C\ i}^{up} \quad \forall i,t,w,k \tag{59}$$

Finally, the linear approximation model of the proposed scheme is as follows:

$$\text{Objective functions } (1) - (3) \tag{60}$$

$$\text{Constraints } (4) - (7), (10), (13) - (14), (17) - (29), (31) - (59) \tag{61}$$

3. Stochastic integrated model

3.1. Proposed single-objective formulation

The problem represented in (60)-(61) is in the form of a problem with several objective functions. Traditional methods to solve such multi-objective problems attempt to provide a single-objective model so that an optimal solution is obtained for such multi-objective problems. This part of the paper employs the Pareto optimization method based on the sum of weighted functions approach [23]. Equations (62)–(64) express mathematical formulation of the single-objective problem. In this method, the objective function (F) as in (62) will be equal to the sum of the weighted functions of EPC, NEL, and EENS, whose weighting coefficients are ϑ_{EPC}, ϑ_{NEL}, and ϑ_{EENS}, respectively. Choosing values for these weighting coefficients must be subject to (63), meaning that their sum must always be equal to 1. The problem, as in (64), will be bound by the constraints of the multi-objective problem, (61).

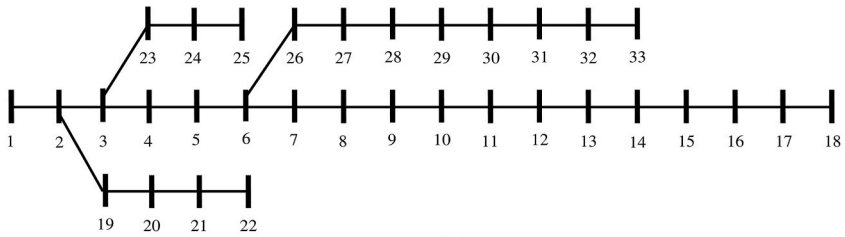

(a)

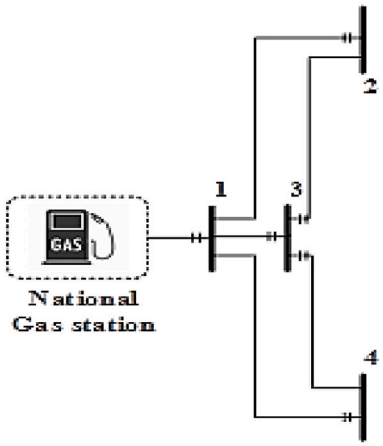

(b)

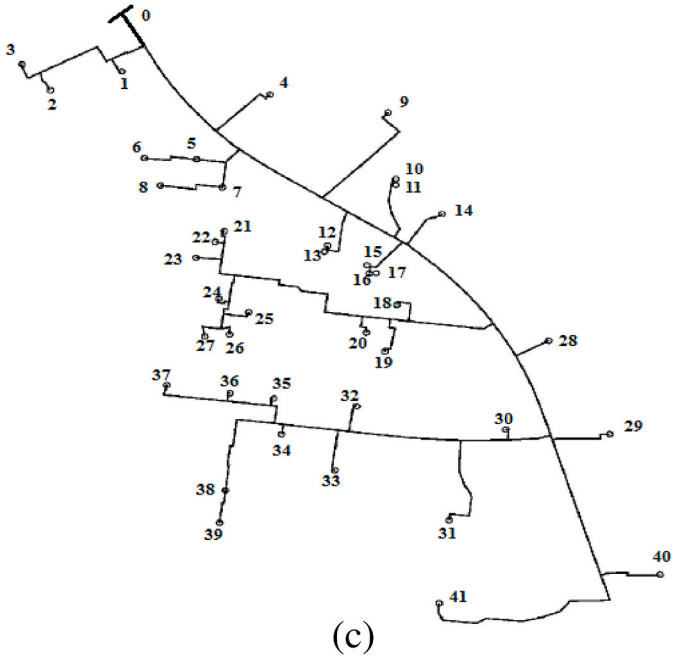

(c)

Fig. 2. Test distribution system, a) 33-bus electrical network [9], b) 4-node gas network [13], and c) 42-node district heating network [24].

$$\min \quad F = \vartheta_{EPC} EPC + \vartheta_{NEL} NEL + \vartheta_{EENS} EENS \tag{62}$$

Subject to:

$$\vartheta_{\mathrm{EPC}} + \vartheta_{\mathrm{NEL}} + \vartheta_{\mathrm{EENS}} = 1 \tag{63}$$

$$\text{Constraint } (61), \text{and EPC, NEL and EENS model in Eqs. } (1) - (3) \tag{64}$$

In the problem described by Eqs. (62)–(64), different values are found for functions EPC, NEL, and EENS for ϑ_{EPC}, ϑ_{NEL} and ϑ_{EENS}. Three-dimension drawing of these values show the Pareto front of the suggested design. So, objective functions need to reach a compromise between their values. In this regard, the fuzzy decision technique (FDT) is used. Description of this technique is provided in Algorithm 1 [19]. In this algorithm, minimum (f^{min}) and maximum (f^{max}) values of EPC, NEL, and EENS are found from (62)-(63) by considering three cases of $\vartheta_{EPC} = 1$, $\vartheta_{NEL} = 1$, and $\vartheta_{EENS} = 1$.

Algorithm 1 Algorithm of the FDT

The compromise solution of a Pareto front;
Pareto optimal solution together with the priorities of the decision-maker;
Step 1: Computation of the Fuzzy membership function
Calculate linear fuzzy membership functions ($\widehat{f}_i$) for individual members of the Pareto optimal front
for i = *EPC*, *NEL*, *EENS*
if $f_i \le f_i^{min}$
The fuzzy membership function ($\widehat{f}$) is 1
elseif $f_i^{min} \le f_i \le f_i^{max}$
The fuzzy membership function is $\frac{f_i - f_i^{\max}}{f_i^{\min} - f_i^{\max}}$;
elseif $f_i \ge f_i^{max}$
The fuzzy membership function is 0;
end
end
Step 2: Obtain α_m
$\alpha_m = \min(\widehat{f}_{EPC}^m, \widehat{f}_{NEC}^m, \widehat{f}_{EENS}^m) \quad \forall m \in \{1, 2, \ldots, n_m\}$
Step 3: The best compromise solution
Find the compromise solution by computing $\max_m \quad \alpha_m$

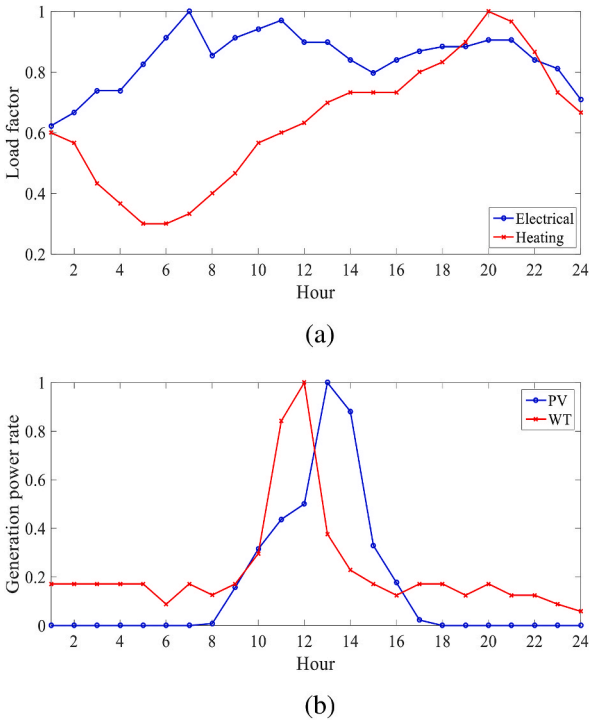

Fig. 3. Daily curve of, a) load factor [9,24], and b) generation power rate of RESs [13].

Algorithm 1. Pseudocode of FDT

3.2. Uncertainty model

Quantities like load (P_L, Q_L, H_L, and G_L), power generation rate of RESs (φ_R), energy price (γ), and energy networks equipment accessibility (u) are uncertainty parameters. These are modeled using the SBSP in this paper. To realize this, the MCS generates many scenarios. In each scenario, the values of uncertainty parameters are found based on their average and standard deviation (s.t) values [13]. The value of energy networks equipment accessibility (u) is calculated according to the forced outage rate (FOR) of the equipment [2]. After that, the probability of the values selected for load and energy price at any given scenario is calculated using a normal probability distribution function (PDF) [13]. The probability values of φ_R and u are found according to the beta (Weibull) and Bernoulli PDFs, respectively [1,2]. Moreover, the probability of a generated scenario (ρ^0) is found by multiplying the probability values of the parameters mentioned in that scenario. As adopting many scenarios in the problem is probable to inhibit the problem from gaining a feasible solution, a scenario-reduction method can be a suitable solution. Here, the Kantorovich method (KM) is used to this purpose, in which a given number of the scenarios with minimum distance from each other is selected [5]. The probability of a selected scenario (ρ) is equal to the ratio between ρ^0 of that scenario and the sum of ρ^0 of the scenarios selected by the KM.

4. Numerical results and discussion

4.1. Case study

Fig. 2 shows the test system that consists of a 33-bus electrical distribution network [9], a 4-node gas distribution network [13], and a 42-node thermal district heating system [24]. The information and data of the networks including peak load data, distribution line and pipeline characteristics, and data of distribution substations can be extracted from Refs. [9,13,24]. The base power and voltage values of the electricity network are 1 MVA and 12.66 kV, respectively. The base power and pressure in the gas network are set 1 MW and 10 bar, respectively. The base power and base temperature of the heating network are 1 MW and 100^0C. The permissible voltage, temperature, and pressure values are within [0.9 1.1] p.u. The gas power is transformed to electrical and thermal power, and the amount of passive gas charge, G_L, is zero. Hourly load (active, reactive, and thermal) is found by multiplying the peak load and the daily load factor curve. Fig. 3(a) illustrates such a curve for electrical and heating networks [9,24]. The coincidence factor (*CF*) [1] is set 0.7. Referring to Ref. [13], the price of electrical energy at 1:00–7:00; 8:00–16:00 and 23:00–00:00; and 17:00–22:00 is 17.6 $/MWh, 26.4 $/MWh, and 33 $/MWh, respectively. The price of heating energy during 5:00–15:00 is 30 $/MWh, and for other hours is 22 $/MWh. Concerning the gas network, the gas price during 1:00–5:00 and 23:00–00:00 is 12 $/MWh, while it is 18 $/MWh in other intervals.

EHs can be equipped with batteries as EESs; TESs; PVs and wind turbines (WTs) as RESs; boilers; and CHPs. The load of individual EHs (as shown in Fig. 2) can participate in the DRP at a rate of 40 %. The EH load in this case is equal to the load located in an electricity bus or gas/heating node in which there is an EH. The maximum size of a PV (WT) is set 0.5 MW, with overall capital cost of 2.5 M$/MW (3.2 M$/MW) [25]. Fig. 3(b) depicts the expected daily curve of the power generation rate of RESs (φ_R) [13]. The CHP with a maximum capacity of 1 MVA and a total capital cost of 2.5 M$/MVA can be positioned in EHs. In the CHP, parameters η_T, η_L, η_H and ϖ are set 0.4, 0.09, 0.4, and 0.52, respectively [19]. The boiler with operation efficiency of 80 % has a maximum capacity of 1 MW and its installation cost is 1.5 M$/MW [13]. The battery with charge/discharge efficiency of 90 % can have a maximum capacity of 2 MWh with a total capital cost of 2 M$/MWh [25]. The charge and discharge intervals are considered 2.5 h, and parameters υ and ν are set 0.1. Such data for TESs are given except for that their charging and discharging efficiency is set 80 %, and the total installation cost is 1.75 M$/MWh. The occurrence of fault in a 10-year planning horizon may cause an interruption interval of 30 days ($du = 30$). FOR is set 1 % for all elements of electricity, gas and heating networks [2]. Standard deviation of uncertainties associated with load, energy price, and renewable power is set 10 %. MCS produces 2000 scenarios and KM applies 50 scenarios to the problem. ΔF is considered 0.05 p.u. to achieve high flexibility in EHs.

4.2. Results

Simulation of the suggested scheme in this paper is implemented using the GAMS optimization software [26], which follows the data given in subsection 4.1. The proposed scheme includes the mathematical formulation [27–31]. This formulation is based on the

Table 2
Pareto front of the proposed scheme for ΔF = 0.05 p.u.

ϑ_{EPC}	ϑ_{NEL}	ϑ_{EENS}	EPC (M$/year)	NEL (MWh)	EENS (MWh)
1	0	0	11.95	2964.72	57.34
0	1	0	14.32	2257.34	23.47
0	0	1	15.87	2578.41	11.46
0.5	0.5	0	13.14	2386.92	27.11
0.5	0	0.5	13.67	2613.22	15.75
0	0.5	0.5	14.98	2365.48	13.89
0.33	0.33	0.33	14.02	2405.36	14.63

optimization method [32–36]. The optimization model includes the objective function [37–41]. Objective function minimizes or maximizes a function [42–46]. The optimization formulation contains the different constraints [47–51]. Constraints includes equality and inequality equations [52–54]. To apply the optimization model on the energy networks, it is needed to use the smart systems [55–59]. These systems include Telecommunications equipment [60–64]. The following provides a summary of the obtained results through simulations.

A) *Achieving a compromise solution using the appropriate solution algorithm*: This section analyzes the convergence results of the proposed scheme for $\Delta F = 0.05$ p.u. First, the Pareto front of the scheme for four values of 0, 0.33, 0.5, and 1 for weighting coefficients of ϑ_{EPC}, ϑ_{NEL}, and ϑ_{EENS} is reported in Table 2. The minimum and maximum values of objective functions EPC, NEL, and EENS are specified for three cases of $\vartheta_{EPC} = 1$, $\vartheta_{NEL} = 1$, and $\vartheta_{EENS} = 1$. These values for EPC are 11.95 M$/year and 15.87 M$/year. For NEL, these values are 2257.34 MWH and 2967.72 MWh. And, for EENS, they are 11.46 MWh and 57.34 MWh. The range of changes for each function is equal to the difference between the minimum and maximum values of that function. Therefore, for EPC, NEL, and EENS, the range of changes is respectively 3.92 M$/year, 710.38 MWh, and 45.88 MWh. Table 2 shows that the trends of changes (in terms of increase or decrease) of the mentioned three objective functions are not in the same direction. To elucidate on, the decrease in EENS corresponds with the increase in EPC because to reduce the interruption of customers or to reduce EENS, the customers need to be supplied at the demand side. Hence, a higher number of local power sources such as EHs are required to be built in energy networks. Since the increase in the number of EHs equally means the increase in their installation cost, the EPC increases under such conditions. As another point. The reduction in NEL corresponds with the increase in the EPC because the increasing the number of EHs up to a certain number leads to a reduction in the amount of energy demand by customers from the upstream network, leading to reduced power and energy loss. Also, based on Table 2, the reduction in EENS equals the increase in the NEL. The reason is that as the number of EHs or local sources increases, the possibility of outage of customers in the case of an $N-1$ event decreases. However, significant increase in the number of EHs in energy networks guides the power flow through the distribution lines from EH side toward the upstream network. This is in accordance with the increase in the power and energy loss.

In order to derive a compromise solution between EPC, NEL, and EENS functions, in this paper, fuzzy decision-making technique was used, the results of which are reported in Table 3. These results are expressed for the nonlinear model, (62)–(63), constraints (4)–(49), linear model, (62)–(64), and the proposed design. IPOPT, CONOPT, LGO, and MINOS solvers [26] have been used to solve the nonlinear model. According to Table 3, among these algorithms, only two algorithms, IPOPT and CONOPT, have the optimal solution, and the other algorithms were not able to extract the optimal solution. IPOPT and CONOPT also have different solutions, in other words, they do not have a single solution. Also, its computational time is more than 2450 s. As a point, among the solvers of the nonlinear model, the algorithm with a more efficient solution and lower computational time is desirable [16]. This is true for IPOPT because it has the lowest values of EPC, NEL, and EENS functions compared to CONOPT, and its computational time is lower. In the linear model, CPLEX, CBC, and OSL algorithms [26] are used to solve the problem. According to Table 3, the values of the mentioned objective functions are the same for all three algorithms, so the linear model solvers have a unique solution. Also, their computational time is less than 150 s, which is much lower than IPOPT results. This situation is more favorable for CPLEX because it has the shortest computational time of 125.6 s. It is noteworthy that based on [6,13,15], the computational error of the variables of electric power (active and reactive), gas power, heat power, voltage, pressure, and temperature in the linear model compared to the nonlinear model is about 2.5 %, 0.9 %, 0, 0.5 %, 0.1 %, and 0. However, this computational error can be neglected due to the very low computational time and the possibility of access to a unique solution. Note that the compromise point in the linear and nonlinear models is different because the optimal solution extracted for them is different. As another point to note, by comparing the results reported in Tables 2 and 3, it is observed that at the compromise point, the CPLEX algorithm, $\vartheta_{EPC} = 0.7$, $\vartheta_{NEL} = 0.15$, and $\vartheta_{EENS} = 0.08$, the values of the mentioned objective functions are close to their minimum values. For instance, the EPC is about 28.5 % ((13.08–11.95)/3.92) distant from its minimum value. This value for NEL and EENS is 16.3 % and 4.2 %.

B) *Analysis of planning and operation results of EHs*: Table 4 lists the planning results of EHs in electrical, gas, and heating networks for the compromise point obtained in Table 3 for $\Delta F = 0.05$ p.u. Table 4 shows that the system (Fig. 2) should contain 10 EHs so that its technical and economic indicators are enhanced. EHs 1 to 5 are located only in the electrical network with no connection to gas and heating networks. The EHs contain WTs, PVs, and battery storage elements. As these are present only in the electrical network, the DRP is implemented on the active load. The capacity of WTs and batteries for EHs 1 to 5 is the same so that the maximum sizes of WTs and batteries are found using the data in subsection 4.1. In the case of PVs, a PV with a maximum size of 0.5 MW is located in some EHs. In some other EHs, a PV with a smaller size (0.4 MW) is positioned. This can be explained as follows. First, as Fig. 3 shows, PVs are often switched off and their capital cost is significant. So, adopting a large size PV is not economically justified.

Table 3
Compromise solution obtained by different solvers for $\Delta F = 0.05$ p.u.

Model	Solver	CI	CT (sec)	ϑ_{EPC}	ϑ_{NEL}	ϑ_{EENS}	EPC (M$/year)	NEL (MWh)	EENS (MWh)	Model status
Non-linear	IPOPT	562	2472.1	0.75	0.18	0.07	13.92	2443.65	14.56	Feasible
	CONOPT	691	2923.6	0.76	0.17	0.07	14.09	2489.32	14.78	Feasible
	LGO			–						Infeasible
	MINOS			–						Infeasible
Linear	CPLEX	112	125.6	0.77	0.15	0.08	13.08	2373.22	13.37	Feasible
	CBC	135	134.1	0.77	0.15	0.08	13.08	2373.22	13.37	Feasible
	OSL	167	146.2	0.77	0.15	0.08	13.08	2373.22	13.37	Feasible

Table 4
Planning results of EHs in electrical, gas and heating networks for ΔF = 0.05 p.u.

EH	EH location			RES size (MW)		EES size (MWh)	CHP size (MVA)	Boiler size (MW)	TES size (MWh)
	En	*tn*	*Gn*	PVs	WT	Battery			
1	7	–	–	0.5	0.5	2	0	0	0
2	13	–	–	0.4	0.5	2			
3	16	–	–	0.4	0.5	2			
4	26	–	–	0.4	0.5	2			
5	30	–	–	0.5	0.5	2			
6	4	5	3	0.5	0.5	2	1		1.5
7	19	41	2	0.5	0.5	2	1		1.5
8	18	20	4	0	0	0	1	1	2
9	24	33	2				1	1	2
10	32	14	3				1	1	2

Second, the operating constraints of electrical network, (12), (15)–(16), rejects employing large-scale EHs. As a result, the EH operator mostly incorporates small PVs. EHs 6–10 are connected to each of electrical, gas, and heating networks. In EH 6–7, besides RESs, EESs, and electric DRPs, there exists CHP, TES, and thermal DRP as well. The size of electrical sources and storage devices in these EHs are the same as EHs 1–5. The maximum size of the CHP (1 MVA) is chosen for EHs 6–10. Regarding the notes given in subsection 4.1, the price of gas energy in most intervals is less than the price of electricity and heat. Hence, to minimize the operating cost of EHs (second term of EPC), it is advised to adopt CHP to meet the thermal and electrical demand. CHPs with maximum size are located in EHs 6–10. EHs 6–7 lack any boilers, whereas a 1.5 MWh TES is installed. A 1 MW boiler is placed at EHs 8–10, and the size of TES is 2 MWh, where no electrical source or storage is connected to these EHs. Considering that EHs 6–10 are located in electrical and thermal buses, the DRP in these EHs can be of both electrical and thermal type. The storage size is found based on the power source size [20]. As the heat source size is larger in EHs 10-8 compared to that in EHs 6–7, the TES size is larger in EHs 8–10. Note that the location and size of EHs is proportional to improving the economic situation and flexibility of EHs besides enhancing the operation and reliability status of energy networks.

The economic planning results of EHs listed in Table 4 are reported in Table 6 for ΔF = 0.05 p.u. As is observed, the capital cost of ten EHs in the 10-year planning horizon is 90.34 M$. The overall operating cost of these EHs in the planning horizon reaches roughly 19.96 M$. So, the EH planning cost (including capital cost and operating cost) is 110.3 M$. Nonetheless, as per Table 5, there is no operating cost for EHs 1 to 5, even though they sell active power to the electrical network and gain financial benefit. Thus, their operating cost has a negative value. Concerning EHs 6–10, CHP and EHs are gas energy consumers. Electric and thermal loads are also available in EHs 6–10. So, EHs 6–10 can inject a small amount of active power and thermal power into electrical and thermal networks, so always imposing operating costs.

The expected daily curve of active, reactive, thermal, and gas power of EHs placed in energy networks for ΔF = 0.05 p.u are illustrated in Figs. 4–6. A negative (positive) value means that power is consumed (generated). As shown in Fig. 4, EHs consume active power during 1:00–7:00 and 16:00 and generate active power in rest of the hours. According to subsection 4.1, the price of electricity is lowest during 1:00–7:00. Thus, to minimize the operating cost of EHs, storage devices and responsive loads in this interval are charged and receive active power from the electrical network. Moreover, PVs are generally switched off in these intervals, and PVs and WTs produce low power at hour 16:00. So, the active power of EHs in this period has a negative value. During the rest of intervals, power sources like WTs and PVs feed higher amounts of active power, while EESs and electric DRPs operating in discharge mode feed active power into the networks. Consequently, the active power generation of EHs in these intervals has a positive value, showing that EHs can produce electrical power. Fig. 4 depicts the expected daily curve of reactive power produced by all EHs. As is shown, EHs inject

Table 5
Economic results of EHs planning in different energy networks for ΔF = 0.05 p.u.

EH	Total installing cost in planning horizon (M$)						Operation cost (M$)
	PVs	WT	Battery	CHP	Boiler	TES	
1	2.6	1.6	4	0	0	0	−0.83
2	2.08	1.6	4				−0.51
3	2.08	1.6	4				−0.49
4	2.08	1.6	4				−0.53
5	2.6	1.6	4				−0.85
6	2.6	1.6	4	2.5		3.5	3.92
7	2.6	1.6	4	2.5		3.5	3.87
8	0	0	0	2.5	1.5	3.5	5.12
9				2.5	1.5	3.5	5.15
10				2.5	1.5	3.5	5.11
Total	16.64	11.2	28	12.5	4.5	17.5	19.96
Total investment cost (M$)	90.34						–
Total planning cost (M$)	110.3						

Table 6
Improving different indices in Case II in comparison to Case I.

Parameter		Case I	Case II		
			ΔF = 0 p.u.	ΔF = 0.05 p.u.	ΔF = 0.1 p.u.
EENS (MWh) in network of	Electrical	251.4	6.38	6.32	6.18
	Gas	0	0	0	0
	Heating	290.2	7.11	7.05	6.77
Total EENS (MWh)		541.6	13.49	13.37	12.95
NEL (MWh) in network of	Electrical	1622.1	931.74	920.43	887.66
	Gas	0	329.51	329.51	329.51
	Heating	1891.3	1147.23	1123.28	1095.39
Total NEL (MWh)		3513.4	2408.48	2373.22	2312.56
Maximum drop value of	Voltage (p.u.)	0.087	0.051	0.049	0.046
	Pressure (p.u.)	0	0.046	0.046	0.046
	Temperature (p.u.)	0.093	0.056	0.054	0.051
Maximum over-value of	Voltage (p.u.)	0	0.011	0.013	0.015
	Pressure (p.u.)	0	0	0	0
	Temperature (p.u.)	0	0.014	0.016	0.019

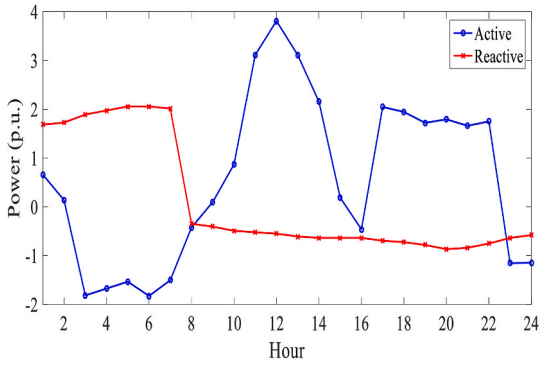

Fig. 4. Expected daily curve of active and reactive of all EHs for ΔF = 0.05 p.u.

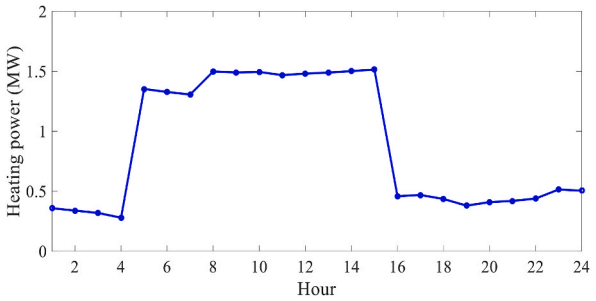

Fig. 5. Expected daily heat power curve of all EHs for ΔF = 0.05 p.u.

high reactive power into the electrical network during 1:00–7:00. The reason is that the active power consumed during these periods is high because of EHs and passive loads (refer to Fig. 2). To inhibit significant voltage drop in these intervals, EHs supply high reactive power into the network. Yet, at the rest of intervals, EHs consume reactive power because active power injection into the electrical network is high. To inhibit overvoltage in the network, the amount reactive power injection into the electrical network by EHs is reduced during 1:00–7:00 so they consume power. Moreover, EHs inject higher heat during peak heat hour (5:00–15:00) than off-peak heat interval, refer to Fig. 5. This is because the thermal energy price is the highest in these intervals. To minimize the operating cost of EHs, TES and thermal DRP need to operate in the discharging mode. The heat power fed into the heating network by EHs is the highest in this interval. In other periods, the thermal energy price is the lowest, so TES and DRP are in the charging operation mode. Fig. 6 demonstrates the expected daily curve of gas power of EHs, in which the gas power of EHs oscillates between −16.2 MW and −18.8 MW, which is due to the fluctuation of active and thermal power of CHPs and the thermal power of boilers considering the performance of other EH elements and passive loads.

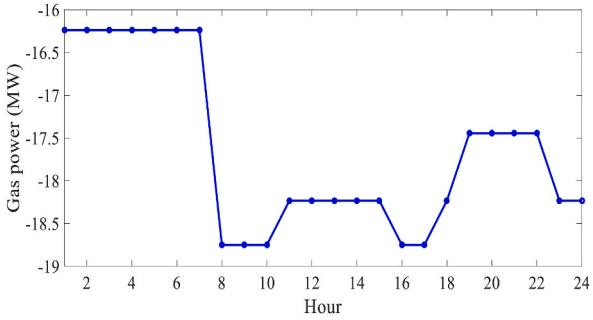

Fig. 6. Expected daily gas power curve of all EHs for ΔF = 0.05 p.u.

C) *Analysis of the operation, reliability and flexibility status of energy networks*: Table 6 lists the operation and reliability indices of energy networks at different conditions of EHs flexibility for two case studies, including power flow studies [65–69] (Case I) and the proposed scheme (Case II). This table also reports the EENS, NEL, maximum overvoltage or voltage drop, pressure, and temperature for different case studies with different value of ΔF. As per this table, the EENS for the electrical and thermal networks is about 251.4 and 290.2 MWh in Case I. EENS is zero for gas network because it is assumed that CHP and boilers (EHs) are the only gas energy consumers while they are not available in Case I. Hence, the sum of EENS (as a reliability index) in the system for Case I is approximately 541.6 M$/year. In the proposed scheme (Case II), by selecting the optimal site and capacity for power sources and ESSs, the EENS at ΔF = 0 (100 % flexibility of EHs) for electricity and heating networks is reduced to roughly 6.38 MWh and 7.11 MWh, respectively. However, it is zero for the gas network. So, the total value of EENS for Case II at ΔF = 0 is 13.49 MWh, showing almost 97.5 % ((541.6–13. 49)÷541.6) reduction in comparison with Case I. The EENS, based on (21)-(23) and Tables 6 and is nonzero only for electrical and thermal networks and is zero for gas network because, the present study assumes that the passive gas demand, G_D, is zero. This demonstrates that the suggested scheme can achieve high reliability for energy networks with EHs in the case of an $N-1$ contingency. Based on Table 4, EHs are generally distributed in different consumption buses (nodes) of energy networks and can supply the lost sources during an interruption. The same is true for NEL (operation index). In Case I, based on Table 6, the NEL for electric, gas, and heating networks is 1622.1 MWh, 0 MWh, and 1891.3 MWh, respectively, resulting in NEL of about 3513.4 MWh. This parameter in Case II for ΔF = 0 is 931.74 MWh, 329.51 MWh, and 1147.23 MWh for the networks, respectively, and the total NEL in these conditions is 2408.48 MWh. Therefore, by increasing the yearly energy loss of 329.51 MWh in the gas network compared to Case I, the proposed scheme has reduced NEL by about 6.42 % and 39.3 % in electrical and heating networks compared to Case I. Thus, the total NEL in Case II for ΔF = 0 is decreased by roughly 31.4 % in comparison with Case I.

Table 6 shows the maximum and minimum values of voltage, pressure, and temperature (operation indices) for cases I and II. As is seen, in Case I, the maximum voltage drop and temperature is 0.087 p.u. and 0.093 p.u., but the maximum pressure drop is 0. Concerning Case I that contains electric and thermal consumers, there is a drop in voltage and temperature, but the pressure is not changing. In Case II at ΔF = 0, using the optimal planning and operation of power sources, ESSs, and responsive loads in the form of an EH, the highest decrease in voltage and temperature are 0.051 p.u. and 0.056 p.u., respectively. The maximum pressure drop is increased to 0.046 p.u. compared to Case I. As per Table 6, there is no over-voltage, over-temperature, and over-pressure in Case I. In Case II with ΔF = 0, the maximum over-voltage and over-temperature are 0.011 p.u. and 0.014 p.u., but they are lower than their limit, i.e. 0.1 (1.1 - 1) p.u. [70–74]. So, by establishing a maximum pressure drop of 0.046 p.u., a maximum over-voltage of 0.011 p.u., and a maximum over-temperature of 0.014 p.u., the proposed scheme in Case II with ΔF = 0 improves the voltage and temperature by about 41.4 % and 39.8 % compared to Case I. In the end, with increasing ΔF, the importance of flexibility is reduced in the proposed scheme based on constraints (48) and (49). Hence, the performance of power sources, ESSs, and responsive loads is mostly toward improving the economic status of EHs and operation and reliability status of energy networks. So, with increased ΔF, values of EENS, NEL, voltage drop, and temperature drop decrease.

5. Conclusion

This research addresses the optimal planning and operation of power sources and ESSs in the form of flexible grid-connected EHs with responsive loads subject to the reliability of electrical, gas, and heating networks. A three-objective optimization modeling is used to state the problem in which objective functions try to find the minimum values of expected annual planning cost of EHs, expected annual energy losses of electricity, gas, and heating networks, and EENS during an $N-1$ event. The design was limited by optimal power flow equations of energy networks, reliability constraints of these networks, planning and operation model of EHs, and flexibility limit of EHs. The Pareto optimization is used to establish a single-objective model for the proposed scheme using the sum of weighted functions method. Also, the linear approximation model of the scheme is found, and the uncertainties related to load, energy prices, renewable power, and availability of energy networks elements are modeled using the SBSP. Finally, based on the extracted numerical results, it was observed that the linearized model of the proposed design has a unique optimal solution compared to its

original nonlinear model, which can be solved in very low computational time, especially by using the CPLEX algorithm. Also, in accordance with the optimal planning of EHs to achieve the desired operation and reliability state of energy networks, in addition to achieving the minimum planning cost for EHs, EHs are installed at different bases (nodes) at the beginning, middle, and the end of the feeder. Then, by extracting the optimal power daily curve for EHs, it was observed that the proposed scheme is able to improve the reliability of power flow distribution studies by about 97 %. Moreover, concerning operating indices such as energy losses, maximum voltage drop, and maximum temperature drop, the suggested scheme in terms of maximum flexibility ($\Delta F = 0$) is able to improve these indices by about 31 %, 41 %, and 40 % compared to power flow studies. Of course, in these conditions, there is a pressure drop, overvoltage, and overheating, but the amount is less than their permissible limit of 0.1 p.u.

Data availability

The data used to support the findings of this study are included within the article.

Funding statement

The authors received no financial support for the research, authorship and publication of this article.

CRediT authorship contribution statement

Abdolhamid Rahideh: Writing – review & editing, Writing – original draft, Validation, Software, Project administration, Methodology, Investigation, Formal analysis, Data curation, Conceptualization. **Mehrdad Mallaki:** Writing – review & editing, Visualization, Validation, Data curation, Conceptualization. **Mojtaba Najafi:** Writing – review & editing, Visualization, Validation. **Abdolrasul Ghasemi:** Writing – review & editing, Visualization, Validation.

Declaration of competing interest

The authors declare that they have no known competing financial interests or personal relationships that could have appeared to influence the work reported in this paper.

References

[1] Z.-Z. Wu, Y.-P. Xu, Z.-L. Cheng, H.-W. Sun, B. Papari, S.S. Sajadi, F. Qasim, Optimal placement and sizing of the virtual power plant constrained to flexible-renewable energy proving in the smart distribution network, Sustain. Energy Technol. Assessments 49 (2022) 101688.
[2] M. Roustaee, A. Kazemi, Multi-objective stochastic operation of multi-microgrids constrained to system reliability and clean energy based on energy management system, Elec. Power Syst. Res. 194 (2021) 106970.
[3] E. Faraji, A.R. Abbasi, S. Nejatian, M. Zadehbagheri, H. Parvin, Probabilistic planning of the active and reactive power sources constrained to securable-reliable operation in reconfigurable smart distribution networks, Elec. Power Syst. Res. 199 (2021) 107457.
[4] A. Azarhooshang, D. Sedighizadeh, M. Sedighizadeh, Two-stage stochastic operation considering day-ahead and real-time scheduling of microgrids with high renewable energy sources and electric vehicles based on multi-layer energy management system, Elec. Power Syst. Res. 201 (2021) 107527.
[5] A. Jamali, J. Aghaei, M. Esmaili, A. Nikoobakht, T. Niknam, M. Shafie-khah, J.P.S. Catalão, Self-scheduling approach to coordinating wind power producers with energy storage and demand response, IEEE Trans. Sustain. Energy 11 (2019) 1210–1219.
[6] H. Zafarani, S.A. Taher, M. Shahidehpour, Robust operation of a multicarrier energy system considering EVs and CHP units, Energy 192 (2020) 116703.
[7] L.D.L. Pereira, I. Yahyaoui, R. Fiorotti, L.S. de Menezes, J.F. Fardin, H.R.O. Rocha, F. Tadeo, Optimal allocation of distributed generation and capacitor banks using probabilistic generation models with correlations, Appl. Energy 307 (2022) 118097.
[8] A. Naderipour, S.A. Nowdeh, P.B. Saftjani, Z. Abdul-Malek, M.W. Bin Mustafa, H. Kamyab, I.F. Davoudkhani, Deterministic and probabilistic multi-objective placement and sizing of wind renewable energy sources using improved spotted hyena optimizer, J. Clean. Prod. 286 (2021) 124941.
[9] A. Shahbazi, J. Aghaei, S. Pirouzi, T. Niknam, V. Vahidinasab, M. Shafie-khah, J.P.S. Catalão, Holistic approach to resilient electrical energy distribution network planning, Int. J. Electr. Power Energy Syst. 132 (2021) 107212.
[10] A. Valencia, R.A. Hincapie, R.A. Gallego, Optimal location, selection, and operation of battery energy storage systems and renewable distributed generation in medium–low voltage distribution networks, J. Energy Storage 34 (2021) 102158.
[11] M. Jalili, M. Sedighizadeh, A.S. Fini, Stochastic optimal operation of a microgrid based on energy hub including a solar-powered compressed air energy storage system and an ice storage conditioner, J. Energy Storage 33 (2021) 102089.
[12] P. Wen, Y. Xie, L. Huo, A. Tohidi, Optimal and stochastic performance of an energy hub-based microgrid consisting of a solar-powered compressed-air energy storage system and cooling storage system by modified grasshopper optimization algorithm, Int. J. Hydrogen Energy 47 (2022) 13351–13370.
[13] A. Dini, S. Pirouzi, M. Norouzi, M. Lehtonen, Grid-connected energy hubs in the coordinated multi-energy management based on day-ahead market framework, Energy 188 (2019) 116055.
[14] A. Tavakoli, A. Karimi, M. Shafie-khah, Optimal probabilistic operation of energy hub with various energy converters and electrical storage based on electricity, heat, natural gas, and biomass by proposing innovative uncertainty modeling methods, J. Energy Storage 51 (2022) 104344.
[15] K. Afrashi, B. Bahmani-Firouzi, M. Nafar, IGDT-based robust optimization for multicarrier energy system management, Iranian Journal of Science and Technology, Transactions of Electrical Engineering 45 (2021) 155–169.
[16] M. AkbaiZadeh, T. Niknam, A. Kavousi-Fard, Adaptive robust optimization for the energy management of the grid-connected energy hubs based on hybrid meta-heuristic algorithm, Energy 235 (2021) 121171.
[17] H. Hamidpour, J. Aghaei, S. Dehghan, S. Pirouzi, T. Niknam, Integrated resource expansion planning of wind integrated power systems considering demand response programmes, IET Renew. Power Gener. 13 (2019) 519–529.
[18] D.G. Photovoltaics, E. Storage, IEEE Application Guide for IEEE Std 1547™, IEEE Standard for Interconnecting Distributed Resources with Electric Power Systems, IEEE Std, 2009, pp. 1542–1547.
[19] R. Homayoun, B. Bahmani-Firouzi, T. Niknam, Multi-objective operation of distributed generations and thermal blocks in microgrids based on energy management system, IET Gener. Transm. Distrib. 15 (2021) 1451–1462.
[20] S. Pirouzi, M. Zaghian, J. Aghaei, H. Chabok, M. Abbasi, M. Norouzi, J.P. Catalão, Hybrid planning of distributed generation and distribution automation to improve reliability and operation indices, International Journal of Electrical Power & Energy Systems 135 (2022) 107540.

[21] Sabzalian, M. H., Pirouzi, S., Aredes, M., Wanderley Franca, B., & Carolina Cunha, A. (2022). Two-layer coordinated energy management method in the smart distribution network including multi-microgrid based on the hybrid flexible and securable operation strategy. *International Transactions on Electrical Energy Systems, 2022*.

[22] M. Norouzi, J. Aghaei, S. Pirouzi, T. Niknam, M. Fotuhi-Firuzabad, M. Shafie-khah, Hybrid stochastic/robust flexible and reliable scheduling of secure networked microgrids with electric springs and electric vehicles, Applied Energy 300 (2021) 117395.

[23] W. Jakob, C. Blume, Pareto optimization or cascaded weighted sum: a comparison of concepts, Algorithms 7 (2014) 166–185.

[24] I. Gabrielaitienė, B. Bøhm, B. Sundén, Dynamic temperature simulation in district heating systems in Denmark regarding pronounced transient behaviour, J. Civ. Eng. Manag. 17 (2011) 79–87.

[25] A. Maleki, A. Askarzadeh, Optimal sizing of a PV/wind/diesel system with battery storage for electrification to an off-grid remote region: a case study of Rafsanjan, Iran, Sustain. Energy Technol. Assessments 7 (2014) 147–153.

[26] Generalized Algebraic Modelling Systems (GAMS). [Online]. Available: http://www.gams.com.

[27] J. Song, A. Mingotti, J. Zhang, L. Peretto, H. Wen, Accurate Damping Factor and Frequency Estimation for Damped Real-Valued Sinusoidal Signals, IEEE Transactions on Instrumentation and Measurement 71 (2022) 1–10.

[28] B. Shao, et al., Power coupling analysis and improved decoupling control for the VSC connected to a weak AC grid, International Journal of Electrical Power & Energy Systems 145 (2022) 108645.

[29] Z. Lu, et al., Cooperative Operation of Distributed Energy Resources and Thermal Power Plant With a Carbon-Capture-Utilization-and-Storage System, IEEE Transactions on Power Systems 39 (2024) 1850–1866.

[30] Y. Mao Y. Zhu Z. Tang Z. Chen, A Novel Airspace Planning Algorithm for Cooperative Target Localization, Electronics. 11 (2022) 2950.

[31] P. Li, J. Hu, L. Qiu, Y. Zhao, B.K. Ghosh, A Distributed Economic Dispatch Strategy for Power–Water Networks, IEEE Transactions on Control of Network Systems 9 (2022) 356–366.

[32] J. Mei, K. Li, A. Ouyang, K. Li, A Profit Maximization Scheme with Guaranteed Quality of Service in Cloud Computing, IEEE Trans. Computers. 64 (2015) 3064–3078.

[33] K. Li, W. Yang, K. Li, Performance Analysis and Optimization for SpMV on GPU Using Probabilistic Modeling, IEEE Trans. Parallel Distributed Syst. 26 (2015) 196–205.

[34] Y. Xu, K. Li, L. He, L. Zhang, K. Li, A Hybrid Chemical Reaction Optimization Scheme for Task Scheduling on Heterogeneous Computing Systems, IEEE Trans. Parallel Distributed Syst. 26 (2015) 3208–3222.

[35] X. Shi, K. Li, L. Jia, Improved Whale Optimization Algorithm via the Inertia Weight Method Based on the Cosine Function, Journal of Internet Technology 23 (2022) 1623–1632.

[36] J.S. Pan, Z. Fu, C.C. Hu, P.W. Tsai, S.C. Chu, Rafflesia optimization algorithm applied in the logistics distribution centers location problem, Journal of Internet Technology 23 (2022) 1541–1555.

[37] Q. Yang, S.C. Chu, C.C. Hu, J.M.T. Wu, J.S. Pan, Fish Migration Optimization with Dynamic Grouping Strategy for Solving Job-Shop Scheduling Problem, Journal of Internet Technology 23 (2022) 1275–1286.

[38] J.S. Pan, et al., Tumbleweed optimization algorithm and its application in vehicle path planning in smart city, Journal of Internet Technology 23 (2022) 927–945.

[39] C. Liu, K. Li, K. Li, R. Buyya, A new service mechanism for profit optimizations of a cloud provider and its users, IEEE Transactions on Cloud Computing 9 (2017) 14–26.

[40] J. Chen, et al., Dynamic planning of bicycle stations in dockless public bicycle-sharing system using gated graph neural network, ACM Transactions on Intelligent Systems and Technology (TIST) 12 (2021) 1–22.

[41] K. Li, X. Tang, K. Li, Energy-efficient stochastic task scheduling on heterogeneous computing systems, IEEE Transactions on Parallel and Distributed Systems 25 (2013) 2867–2876.

[42] X. Tang, K. Li, M. Qiu, E.H.M. Sha, A hierarchical reliability-driven scheduling algorithm in grid systems, Journal of Parallel and Distributed Computing 72 (2012) 525–535.

[43] M. Yang, Y. Wang, X. Xiao, Y. Li, A Robust Damping Control for Virtual Synchronous Generators Based on Energy Reshaping, IEEE Transactions on Energy Conversion 38 (2023) 2146–2159.

[44] Z. Xiao, et al., Multi-Objective Parallel Task Offloading and Content Caching in D2D-aided MEC Networks, IEEE Transactions on Mobile Computing 12 (2022) 1–12.

[45] B. Cao, et al., Multiobjective 3-D Topology Optimization of Next-Generation Wireless Data Center Network, IEEE Transactions on Industrial Informatics 16 (2020) 3597–3605.

[46] B. Cao, et al., Hybrid Microgrid Many-Objective Sizing Optimization With Fuzzy Decision, IEEE Transactions on Fuzzy Systems 28 (2020) 2702–2710.

[47] M. Hou, Y. Zhao, X. Ge, Optimal scheduling of the plug-in electric vehicles aggregator energy and regulation services based on grid to vehicle, International Transactions on Electrical Energy Systems 27 (2017) e2364.

[48] Y. Duan, Y. Zhao, J. Hu, An initialization-free distributed algorithm for dynamic economic dispatch problems in microgrid: Modeling, optimization and analysis, Sustainable Energy, Grids and Networks 34 (2023) 101004.

[49] M. Shirkhani, et al., A review on microgrid decentralized energy/voltage control structures and methods, Energy Reports 10 (2023) 368–380.

[50] Y. Lei, et al., DGNet: An Adaptive Lightweight Defect Detection Model for New Energy Vehicle Battery Current Collector, IEEE Sensors Journal 23 (2023) 29815–29830.

[51] F. Yu, C. Lu, J. Zhou, L. Yin, K. Wang, A knowledge-guided bi-population evolutionary algorithm for energy-efficient scheduling of distributed flexible job shop problem, Engineering Applications of Artificial Intelligence 128 (2024) 107458.

[52] S. Li, X. Zhao, W. Liang, M.T. Hossain, Z. Zhang, A Fast and Accurate Calculation Method of Line Breaking Power Flow Based on Taylor Expansion, Frontiers in Energy Research 10 (2022) 1–12.

[53] Z. Luo, Knowledge-guided Aspect-based Summarization. 2023 International Conference on Communications, Computing and Artificial Intelligence (CCCAI), 2023, pp. 17–22.

[54] F. Chen, and et al., Complementary fusion of multi-features and multi-modalities in sentiment analysis, arXiv preprint arXiv. 10 (2019) 1-12.

[55] J. Wang, C. Jin, N. Xiong, Q. Tang, G. Srivastava, Intelligent Ubiquitous Network Accessibility for Wireless-Powered MEC in UAV-Assisted B5G, IEEE Transactions on Network Science and Engineering 8 (2021) 2801–2813.

[56] D. Cao, K. Zeng, J. Wang, P. K. Sharma, X. Ma, Y. Liu , BERT-based Deep Spatial-Temporal Network for Taxi Demand Prediction, IEEE Transactions on Intelligent Transportation Systems. 23 (2022) 9442-9454.

[57] Z. Liao, X. Pang, J. Zhang, B. Xiong, J. Wang, Blockchain on Security and Forensics Management in Edge Computing for IoT: A Comprehensive Survey, IEEE Transactions on Network and Service Management 19 (2022) 1159–1175.

[58] W. Li, Z. Chen, X. Gao, W. Liu, J. Wang, Multimodel Framework for Indoor Localization Under Mobile Edge Computing Environment, IEEE Internet of Things Journal 6 (2019) 4844–4853.

[59] W. Li, H. Xu, H. Li, Y. Yang, Pradip Kumar Sharma, Jin Wang, Saurabh Singh, Complexity and Algorithms for Superposed Data Uploading Problem in Networks with Smart Devices, IEEE Internet of Things Journal 7 (2020) 5882–5891.

[60] Z. Liao, J. Peng, J. Huang, J. Wang, J. Wang, Pradip Sharma, Uttam Ghosh, Distributed Probabilistic Offloading in Edge Computing for 6G-enabled Massive Internet of Things, IEEE Internet of Things Journal 8 (2021) 5298–5308.

[61] Z. Luo, H. Xu, F. Chen, Audio Sentiment Analysis by Heterogeneous Signal Features Learned from Utterance-Based Parallel Neural Network, In AffCon@, AAAI (2019) 80–87.

[62] Z. Luo, and et al., Deep learning-based strategy for macromolecules classification with imbalanced data from cellular electron cryotomography, In 2019 International Joint Conference on Neural Networks (IJCNN). (2019) 1-8.

[63] Y. Wang, et al., Identifying Sources of Subsynchronous Resonance Using Wide-Area Phasor Measurements, IEEE Transactions on Power Delivery 36 (2020) 3242–3254.
[64] J. Song, A. Mingotti, J. Zhang, L. Peretto, H. Wen, Fast iterative-interpolated DFT phasor estimator considering out-of-band interference, IEEE Transactions on Instrumentation and Measurement 71 (2022) 1–12.
[65] F. Khalafian, et al., Capabilities of compressed air energy storage in the economic design of renewable off-grid system to supply electricity and heat costumers and smart charging-based electric vehicles, Journal of Energy Storage 78 (2024) 109888.
[66] S. Pirouzi, Network-constrained unit commitment-based virtual power plant model in the day-ahead market according to energy management strategy, IET Generation, Transmission & Distribution 17 (2023) 4958–4974.
[67] M. Norouzi, et al., Bi-level fuzzy stochastic-robust model for flexibility valorizing of renewable networked microgrids, Sustainable Energy, Grids and Networks 31 (2022) 100684.
[68] L. Bagherzadeh, et al., Coordinated flexible energy and self-healing management according to the multi-agent system-based restoration scheme in active distribution network, IET Renewable Power Generation 15 (2021) 1765–1777.
[69] S. Pirpoor, et al., A novel and high-gain switched-capacitor and switched-inductor-based DC/DC boost converter with low input current ripple and mitigated voltage stresses, IEEE Access 10 (2022) 32782–32802.
[70] M. Norouzi, et al., Flexible operation of grid-connected microgrid using ES, IET Generation, Transmission & Distribution 14 (2020) 254–264.
[71] M. Norouzi, and et al., Enhancing distribution network indices using electric spring under renewable generation permission, In 2019 International Conference on Smart Energy Systems and Technologies (SEST), (2019) 1-6.
[72] H. Liang, S. Pirouzi, Energy management system based on economic Flexi-reliable operation for the smart distribution network including integrated energy system of hydrogen storage and renewable sources, Energy 130745 (2024).
[73] S. Pirouzi, J. Aghaei, Mathematical modeling of electric vehicles contributions in voltage security of smart distribution networks, Simulation 95 (5) (2019) 429–439.
[74] H. Kiani, K. Hesami, A. Azarhooshang, S. Pirouzi, S. Safaee, Adaptive robust operation of the active distribution network including renewable and flexible sources, Sustainable Energy, Grids and Networks 26 (2021) 100476.